Catalysis Today xxx (2017) xxx–xxx

Contents lists available at ScienceDirect

Catalysis Today

journal homepage: www.elsevier.com/locate/cattod

Selective synthesis of acetaldehyde from lactic acid on acid zeolites

M.E. Sad, L.F. González Peña, C.L. Padró, C.R. Apesteguía*

Catalysis Science and Engineering Research Group (GICIC), INCAPE (UNL-CONICET) Predio CCT Conicet, Paraje El Pozo, 3000 Santa Fe, Argentina[1]

ARTICLE INFO

Article history:
Received 18 December 2016
Received in revised form 7 March 2017
Accepted 16 March 2017
Available online xxx

Keywords:
Lactic acid
Acetaldehyde
Biomass conversion
Acid zeolites
Green chemistry

ABSTRACT

The gas-phase lactic acid conversion to acetaldehyde was studied on zeolites HMCM22, HZSM5 and NaZSM5 in a plug-flow fixed-bed reactor at 583 K. HMCM22 was a strong Brønsted acid zeolite that yielded 39.7% of lactic acid decarbonylation products (acetaldehyde + CO), but formed significant amounts of coke because of lactic acid oligomerization in the narrow sinusoidal channels of the zeolite. HZSM5 exhibited a high density of Brønsted acid sites (Brønsted/Lewis acid sites ratio of 3.1) and promoted at high rates the lactic acid conversion, mainly to decarbonylation products (acetaldehyde + CO yield = 57.0%) and lactic acid oligomers. NaZSM5 contained mainly Lewis acid sites of intermediate strength (Brønsted/Lewis acid sites ratio of 0.4) that promoted the high-selectivity synthesis of acetaldehyde from lactic acid (acetaldehyde + CO yield = 96.0%) by suppressing the competitive lactic acid oligomerization and coke precursor formation.

1. Introduction

Acetaldehyde (AD) is widely used to produce valuable chemicals such as acetic acid, acetate esters, α,β-unsaturated aldehydes, pentaerythritol, and pyridine bases [1]. It is commercially obtained through the oxidation of ethylene by the Wacker process in strong acid solutions using $PdCl_2$-$CuCl_2$ catalysts or by acetylene hydration promoted by mercury salts [2,3]. This AD production technology involves the use of petroleum-derived raw materials and environmentally harmful catalysts, and thus significant efforts have been made to develop new cleaner and sustainable processes based on biomass-derived feedstocks such as bioethanol [4,5] or lactic acid [6,7].

Lactic acid (LA) is an attractive feedstock for chemical production because of its high reactivity derived from containing two conjugated hydroxyls and one carboxylic group, and can be commercially obtained at low cost by glucose and xylose fermentation [8–10]. Lactic acid has been selected by the U.S. Department of Energy among the 30 best suitable platform molecules for achieving successful biorefinery development [11,12]. The LA conversion network includes the formation of several valuable chemicals and biopolymers, as depicted in Fig. 1. Lactic acid is mainly used for the synthesis of polylactic acid (PLA), a biodegradable polymer that exhibits performance mechanical properties and thermoplastic processability [13]. Catalytic dehydration of lactic acid leads to acrylic acid (AA) while propanoic acid (PA) and pyruvic acid may be obtained by lactic acid reduction and dehydrogenation, respectively. Lactic acid may also produce 2,3 pentanedione (PD) by condensation, and acetaldehyde either by decarbonylation or decarboxylation (Fig. 1).

Due to both the high reactivity of LA and the many competitive LA conversion pathways, the high-selectivity synthesis of LA-derived products is a challenging task. Many solid catalysts have been investigated for selectively promoting LA conversion reactions of Fig. 1, especially for the synthesis of PLA and AA [14–16]. However, very few papers have studied the selective synthesis of acetaldehyde via lactic acid decarbonylation/decarboxylation. Katryniok et al. [6] investigated the LA conversion on silica-supported heteropolyacids and reported maximum yields of 83% for LA decarbonylation products (AD + CO). Zhai et al. [17] obtained high (AD + CO) yields from LA conversion on metal sulfate catalysts, between 86 and 92%. Nevertheless, heteropolyacids and metal sulfates suffered from a rapid deactivation caused by carbon deposition on the strong surface acid sites. The LA conversion to AD was also studied on aluminum phosphates and magnesium aluminate spinels [7,18]. Although the results in literature showed that the reaction is promoted by acid catalysts, knowledge regarding the effect of the acid site nature and strength on catalyst activity and selectivity is clearly lacking. Surprisingly, zeolites have not been investigated so far for the selective synthesis of AD from LA. We decided then to study the AD synthesis from LA on zeolites HMCM22, HZSM5 and NaZSM5 which exhibit different acid prop-

* Corresponding author.
E-mail addresses: capesteg@fiq.unl.edu.ar, capesteg@gmail.com (C.R. Apesteguía).
[1] Website: http://www.fiq.unl.edu.ar/gicic.

http://dx.doi.org/10.1016/j.cattod.2017.03.024
0920-5861/

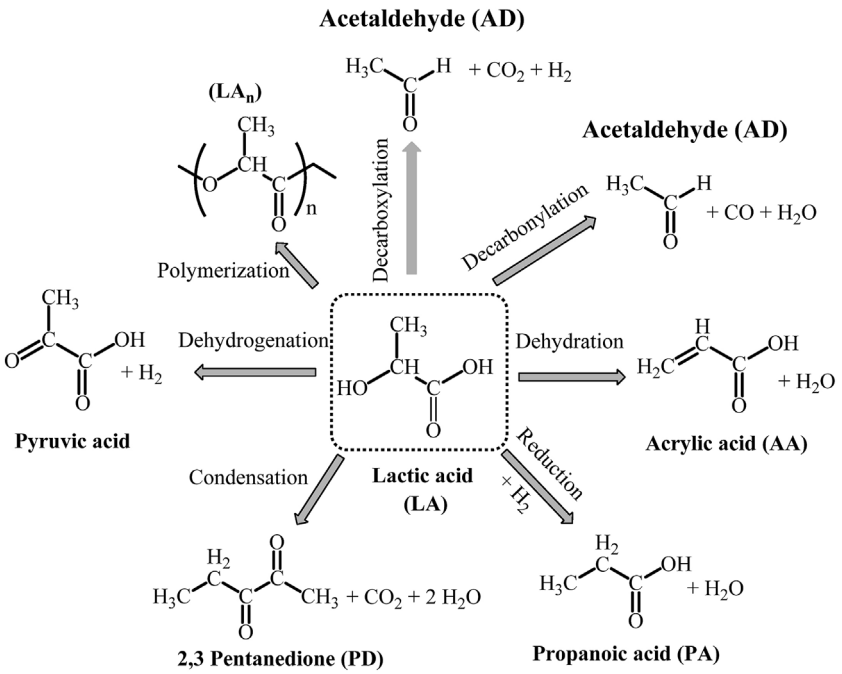

Fig. 1. Lactic acid conversion reactions.

erties. Results are presented in this work and show that the zeolite activity, selectivity and stability for the AD synthesis greatly depend on its acid (acid sites nature and strength) and physical (pore size) properties. In particular, we show here that zeolite NaZSM5 promotes very efficiently the selective synthesis of AD from LA, yielding 96% of LA decarbonylation products (AD + CO) at 583 K.

2. Experimental

2.1. Catalyst preparation

Commercial zeolite NaZSM5 (Zeocat Pentasil PZ-2/25) was calcined at 723 K in dry air flow (60 cm^3/min) for 2 h before use. Zeolite HZSM5 was obtained by exchanging commercial NaZSM5 three times with a 1 M ammonium chloride solution (Merck, 99.8%) at 353 K. Zeolite HMCM22 was synthesized according to [19], by using sodium aluminate (Alfa Aesar, Technical Grade), silica (Aerosil Degussa 380), sodium hydroxide (Merck, >99%), hexamethyleneimine (Aldrich, 99%) and deionized water as reagents. The molar composition of the synthesis gel was $SiO_2/Al_2O_3 = 30$, $OH/SiO_2 = 0.18$, hexamethyleneimine/$SiO_2 = 0.35$ and $H_2O/SiO_2 = 45$. The gel was transferred to a teflon lined stainless steel autoclave, rotated at 50 rpm, and heated to 423 K in an oven for 7–10 days. After crystallization, the solid was washed with deionized water, centrifugated, dried at 373 K, and finally heated in air at 773 K for 15 h.

2.2. Catalyst characterization

Surface areas (S_{BET}) were measured by N_2 physisorption at 77 K in an Autosorb Quantochrome Instrument 1-C sorptometer. Micropore volumes were determined by *t*-plot [20] methods, using the Harkins–Jura equation [21]. Before adsorption, the samples were treated at 623 K under vacuum for 8 h. Elemental compositions were measured using atomic absorption spectroscopy.

The nature, density and strength of surface acid sites of the samples were determined by infrared spectroscopy (IR) in a Shimadzu FTIR Prestige-21spectrophotometer using pyridine as probe molecule, as detailed elsewhere [22]. Samples were ground to a fine powder and pressed into wafers (20–30 mg). The discs were mounted in a quartz sample holder and transferred to an inverted T-shaped Pyrex cell equipped with CaF_2 windows. Samples were initially outgassed in vacuum at 723 K during 2 h and then a background spectrum was recorded after being cooled down to room temperature. Spectra were recorded at room temperature, after admission of pyridine, and sequential evacuation at 423, 573, and 723 K. Spectra were obtained by subtracting the background spectrum recorded previously.

The nuclear magnetic resonance (NMR) spectra for ^{27}Al were recorded at room temperature on a Bruker Avance II 300 spectrometer operating at 78.2 MHz. The sample was spun at the magic angle at a rate of 5 kHz. The ^{27}Al spectrum was recorded using direct polarization with pulses of 1 μs with a repetition time of 2 s. Aluminum chemical shifts are referenced to a 1 M aqueous solution of $Al(NO_3)_3$.

Coke formed on the catalysts during reaction was measured by temperature- programmed oxidation (TPO). Samples (20–50 mg) were heated at 10 K/min in a 2% O_2/N_2 stream from room temperature to 1073 K. The evolved CO_2 was converted into methane by means of a methanation catalyst (Ni/kieselghur) at 673 K and monitored using a flame ionization detector.

2.3. Catalyst testing

The gas-phase conversion of a 35% wt. aqueous solution of lactic acid (Sigma-Aldrich, 85% aqueous solution) was carried out in a fixed-bed flow reactor at 583 K and 101.3 kPa in continuous flow of nitrogen. Samples (particles with 0.35–0.42 mm diameter) were pretreated in-situ in air at 723 K for 2 h before reaction. In a standard catalytic run, the lactic acid solution was fed at 2 ml/h using a syringe pump and vaporized in nitrogen flow (75 ml/min) at 453 K. Catalytic experiments were performed at different contact times (W/F^0_{LA}), between 3.2 and 19.3 g h/mol. The effluent gases from the reactor were passed through a cooled ice/NaCl trap to ensure condensation of acetaldehyde, one of the most volatile reaction products. Liquid products were collected every 30 min and analyzed using a gas chromatograph Agilent 6850 equipped with a flame ionization detector (FID) and a 30-m HP5 capillary

Please cite this article in press as: M.E. Sad, et al., Selective synthesis of acetaldehyde from lactic acid on acid zeolites, Catal. Today (2017), http://dx.doi.org/10.1016/j.cattod.2017.03.024

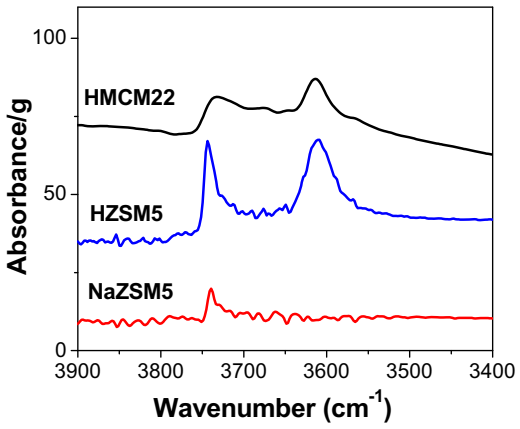

Fig. 2. FT-IR spectra in the hydroxyl stretching region of HMCM22, HZSM5 and NaZSM5.

column (inner diameter: 0.32 mm, film thickness: 0.25 μm). An aqueous solution of isopropyl alcohol (Anedra, 99%) was used as standard to calculate conversions and selectivities. The gaseous products (CO, CO_2 and H_2) were analyzed on line using a Shimadzu 2014 gas chromatograph equipped with a column Hayesep D 100–120 (5 × 1/8 × 2.1 mm), and thermal conductivity (TCD) and flame ionization (FID) detectors. In all the runs, acetaldehyde was not detected in the gas phase. Hydrogen was quantified using the TCD detector while CO and CO_2 were analyzed by FID after completely converting CO and CO_2 to methane by means of a methanation catalyst (Ni/Kieselghur) operating at 673 K. The main reaction products were CO, AD, AA, PA and PD. Linear lactic acid dimer (LA_2), trimer (LA_3) and tetramer (LA_4) were also detected and quantified. The conversion of lactic acid (X_{AL}) was calculated as: $X_{LA} = \left(F^0_{LA} - F_{LA}\right)/F^0_{LA}$, where F^0_{AL} and F_{AL} are the lactic acid molar flow at the inlet and the outlet of reactor, respectively. The carbon-based selectivities (S_j, carbon atoms of product j/carbon atoms of lactic acid reacted) were calculated as $S_j = \alpha_j \cdot F_j/\alpha_{LA} \cdot \left(F^0_{LA} - F_{LA}\right)$, where α_j is the number of C atoms in the product j molecule, F_j is the molar flow of product j, and α_{LA} is the number of C atoms in the lactic acid molecule. The carbon-based yields (Y_j, carbon atoms of product j/carbon atoms of lactic acid fed) were determined as $Y_j = X_{LA}\, S_j$.

3. Results

3.1. Catalyst characterization

The physicochemical and acid properties of the catalysts are shown in Table 1. The specific surface areas of the three zeolites were similar (320–350 m^2/g). No significant modification of S_{BET} was noticed after exchanging the Na^+ cations of NaZSM5 sample by H^+. The degree of exchange of Na^+ cations as determined by atomic absorption spectroscopy was 99.8%. In the Supporting Information, we furnish more information on the zeolite characterization (N_2 adsorption isotherms, t-plots, micropore volumes).

Fig. 2 shows the IR spectra in the hydroxyl stretching region of HZSM5, NaZSM5 and HMCM22 obtained after degassing the sample at 723 K for 4 h. The IR spectrum of the HZSM5 matrix shows two absorption bands at 3610 and 3744 cm^{-1}, respectively. The band at 3610 cm^{-1} corresponds to Si-OH-Al bridging hydroxyl groups [23] whereas the band at 3744 cm^{-1} is attributed to the stretching vibration of terminal SiOH groups located either at the boundaries of the zeolite crystal or at the surface of noncrystalline material [24]. The IR spectrum of zeolite HMCM22 was qualitatively similar to that of HZSM5 showing two absorption bands at similar wavenumbers. In a previous work, we observed that pyridine is strongly adsorbed on

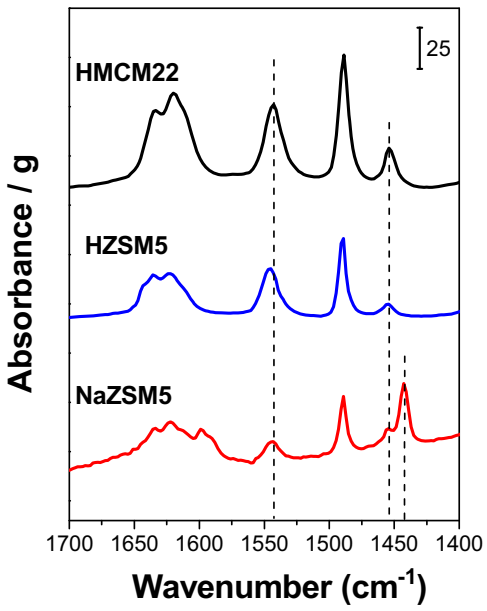

Fig. 3. FTIR spectra obtained after adsorption of pyridine at 298 K and degassing at 423 K.

Si-OH-Al groups at 3610 cm^{-1} while its interaction with terminal silanol OH groups is very weak [25]. The spectrum of degassed zeolite NaZSM5 shows only a small absorption band arising from the SiOH groups at 3740 cm^{-1}.

The nature, density and strength of surface acid sites were determined from the FTIR spectra obtained after admission of pyridine at room temperature and sequential degassing at 423 K, 573 K, and 723 K. The FTIR spectra obtained after pyridine adsorption at 298 K and degassing at 423 K are displayed in Fig. 3. The IR band assignment of the surface species arising from the adsorption of pyridine on acid zeolites has been reported by several authors [26–29]. Pyridinium ions on Brønsted acid sites show absorption bands at 1540 cm^{-1}, 1480–1500 cm^{-1} and 1640 cm^{-1} while pyridine coordinatively bonded on Lewis acid sites gives rise characteristic bands at 1440–1460 cm^{-1}, 1480–1500 cm^{-1} and 1600 cm^{-1}. The relative contribution of Lewis and Brønsted acid sites after evacuation of pyridine at 423 K was obtained then by integration of the bands at 1440–1460 cm^{-1} (PyL, Lewis) and 1540–1545 cm^{-1} (PyH^+, Brønsted). Fig. 3 shows that the PyL band in the IR spectrum obtained on NaZSM5 was split in two overlapping peaks corresponding to pyridine adsorbed on Al (1454 cm^{-1}) and Na (1443 cm^{-1}) Lewis acid sites. The concentration of Brønsted and Lewis acid sites (μmol/g) were quantitatively determined from the area of the characteristic PyL and PyH^+ bands in Fig. 3 and the values of the integrated extinctions molar coefficients (2.22 and 1.67 cm/μmol, respectively) reported in literature for the adsorption of pyridine on acid zeolites [30,31]; results are shown in Table 1. Zeolite HMCM22 contained the highest concentration of Brønsted acid sites (445 μmol/g) and a B/L ratio of 4.2. This latter value is consistent with those reported in literature for zeolites HMCM22 with Si/Al atomic ratios of about 15 [32–34]. The B/L ratio determined for NaZSM5 was 0.4 reflecting a low concentration of Brønsted acid sites (74 μmol/g), as it was suggested by the IR spectrum obtained for NaZSM5 in the OH stretching region (Fig. 2). Zeolite HZSM5 exhibited the lowest concentration of Lewis acid sites (90 μmol/g) and a B/L ratio of 3.6.

Fig. 4 shows the evolution of the amount of pyridine adsorbed on surface Lewis and Brønsted sites as a function of the evacuation temperature and gives insight on the acid site strength. Significant amounts of pyridine remained adsorbed on HMCM22 and HZSM5

Please cite this article in press as: M.E. Sad, et al., Selective synthesis of acetaldehyde from lactic acid on acid zeolites, Catal. Today (2017), http://dx.doi.org/10.1016/j.cattod.2017.03.024

Table 1
Physicochemical and acid properties of the samples.

Catalyst	Physical properties			Acid properties					
				FTIR pyridine (T_{evac} = 423 K)			FTIR pyridine (T_{evac} = 723 K)		
	S_{BET} (m^2/g)	Si/Al	Pore size (Å)	Lewis sites (L) (μmol/g)	Brønsted sites (B) (μmol/g)	B/L	Lewis sites (L) (μmol/g)	Brønsted sites (B) (μmol/g)	B/L
HMCM22	350	15	4.0 × 5.5 4.1 × 5.5	106	445	4.2	54	167	3.1
HZSM5	320	12.5	5.1 × 5.5 5.3 × 5.6	90	323	3.6	47	128	2.7
NaZSM5	330	12.5	5.1 × 5.5 5.3 × 5.6	189	74	0.4	13	2	0.2

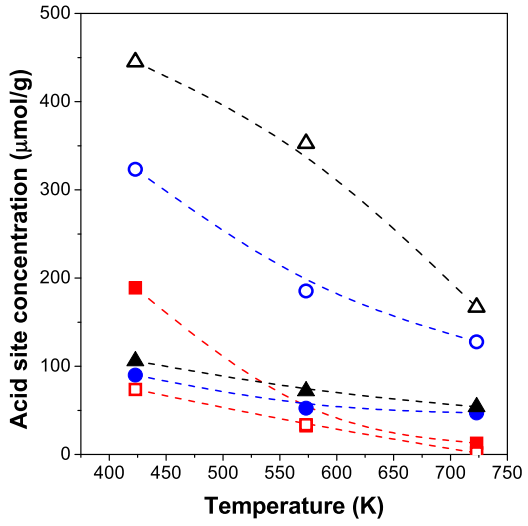

Fig. 4. Concentration of Brønsted (open symbols) and Lewis (closed symbols) acid sites as a function of the evacuation temperature. HMCM22 (△, ▲), HZSM5 (○, ●), NaZSM5 (□, ■).

after evacuation at 723 K revealing the presence of strong Brønsted and Lewis acid sites. The B/L ratios on both zeolites decreased with the evacuation temperature, from 4.2 (423 K) to 3.1 (723 K) on HMCM22, and from 3.6 (423 K) to 2.7 (723 K) on HZSM5 (Table 1). In contrast, the amount of adsorbed pyridine on NaZSM5 readily decreased with the evacuation temperature and was almost completely eliminated after degassing at 723 K, thereby reflecting the moderate acidic character of this zeolite.

3.2. Catalytic tests

The zeolites catalytic performance was initially evaluated at 583 K and a contact time of W/F^0_{LA} = 19.3 g h/mol. This temperature (583 K) was selected because it was the lowest temperature allowing the complete LA conversion at the beginning of the reaction on the three zeolites. Due to the high reactivity of lactic acid, we previously carried out a blank reaction test in absence of catalyst in order to determine the thermal LA conversion at 583 K; a value of X_{LA} = 8% was obtained, being acetaldehyde the main product. The evolution of LA conversion and selectivities as a function of time on stream for the three zeolites are showed in Fig. 5. Results obtained from Fig. 5 by extrapolating the curves at t = 0 are presented in Table 2. Zeolite HMCM22 formed essentially AD by LA decarbonylation producing AD and CO in stoichiometric values, i.e. AD/CO carbon atom ratios close to 2. No CO_2 formed through LA decarboxylation was detected in the gas phase. This zeolite also formed small amounts of AA, PD, LA_3 and LA_4 (the total initial selectivity for all these by-products was less than 6%). The carbon balance (CB) was only 45.3% on HMCM22 (Table 2), thereby indicating that more than half of the carbon atoms fed to the reactor was not detected after reaction in the gas and liquid flows exiting the reactor. The LA conversion on HMCM22 was 100% at the beginning of the reaction but then a continuous activity decay was observed so that X_{LA} was 89% after 4 h on stream (Fig. 5). Zeolite HZSM5 yielded initially 57% of LA decarbonylation products (AD + CO) and significant amounts of LA oligomers, in particular, tetramer (LA_4 = 28%) and trimer (LA_3 = 8.2%). HZSM5 produced also small amounts of PA (2.5%) and PD (1.5%), and traces of AA. In contrast with HMCM22, the carbon balance was very good on HZSM5 at t=0 (CB = 98.4%). Although X_{AL} remained constant at 100%, the AD selectivity slowly decreased with the progress of the reaction and the formation of LA_3 and LA_4 completely disappeared after 100 min on stream (Fig. 5); as a result, the carbon balance decreased to 50.2% at the end of the 4-h run. On zeolite NaZSM5, the selectivity to (AD + CO) was initially 96% (Table 2) and formed traces of AA, LA_3 and LA_4; carbon balance was 97.7%. The lactic acid conversion was complete during the entire catalytic run while the selectivity to (AD + CO) decreased slowly on stream (Fig. 5). At the end of the run, we obtained $S_{(AD+CO)}$ = 88.7%, S_{PD} = 2.1%, and CB = 94.5%.

Coke formed on zeolites was characterized by performing temperature programmed oxidation experiments. Previous to TPO characterization, samples recovered from the catalytic runs showed in Fig. 5 were treated at 523 K in N_2 during 30 min. The obtained TPO profiles are shown in Fig. 6. The TPO curves for HMCM22 and HZSM5 were qualitatively similar and exhibited a broad asymmetric combustion band between 600 K and 970 K with a maximum at about 875 K. NaZSM5 showed a combustion peak at 663 K and a small superimposed oxidation peak at 827 K. The amounts of coke formed during reaction were determined from the area under the TPO curves of Fig. 6 and are included in Table 2 as %C. Significant amounts of coke were formed on HMCM22 (10.8%) and HZSM5 (7.9); the lowest%C value was determined on NaZSM5 (5.2%).

In order to establish the effect of the LA conversion level on product distribution we performed catalytic runs at different contact times (W/F^0_{LA}, g/mol h), between 3.2 and 19.3 g h/mol. In Fig. 7 we plotted the evolution of initial X_{LA} and selectivities as a function of W/F^0_{LA} on HZSM5 and NaZSM5, which according to Fig. 5 promote LA conversion to AD more efficiently than HMCM22. On HZSM5 (Fig. 7A), the (AD + CO) selectivity diminished with W/F^0_{LA} from 74% (W/F^0_{LA} = 3.2 g h/mol) to 57% (W/F^0_{LA} = 19.3 g h/mol). Regarding the evolution of LA oligomers, LA_4 increased while LA_2 decreased as W/F^0_{LA} was increased; LA_3 did not vary significantly with contact time. Minor amounts of PD, PA, and AA were also detected but are not represented in Fig. 7A. The carbon balance was higher than 95% in all the cases. The initial LA conversion rate (r^0_{LA}, mol/g h) was determined from the slope at W/F^0_{LA} = 0 of the X_{LA} curve in Fig. 7A; a value of r^0_{LA} = 0.217 mol/g h was obtained. Zeolite NaZSM5 was highly selective for LA decarbonylation; as shown in Fig. 7B, the (AD + CO) selectivity was about 96%, irrespective of the W/F^0_{LA} value. Minor amounts of PD and LA oligomers were also obtained.

Please cite this article in press as: M.E. Sad, et al., Selective synthesis of acetaldehyde from lactic acid on acid zeolites, Catal. Today (2017), http://dx.doi.org/10.1016/j.cattod.2017.03.024

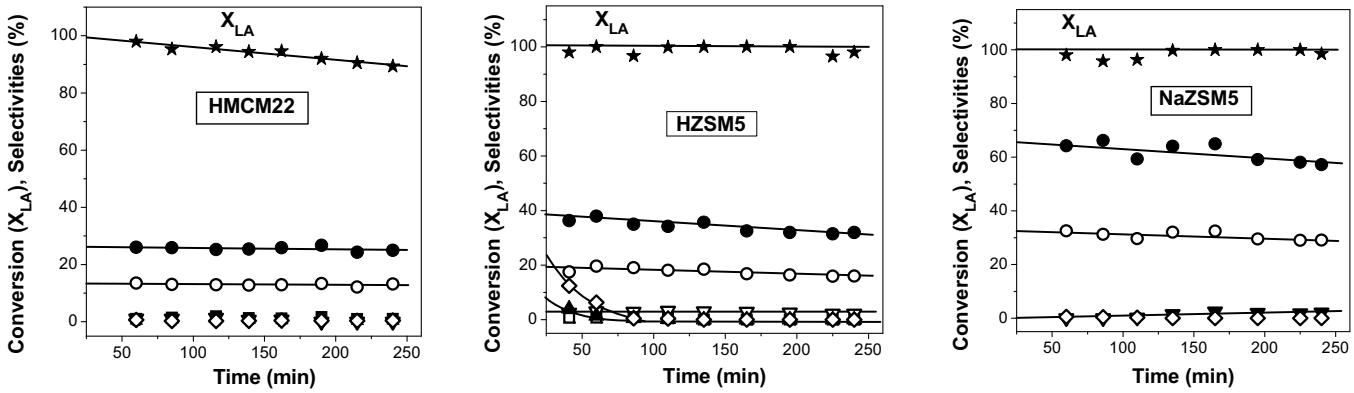

Fig. 5. LA conversion (⋆) and selectivities: AD (●), CO (○), PD (▽), AA (■), PA (▼), LA_2 (□), LA_3 (▲), LA_4 (◊), as a function of time.

Table 2
Catalytic results.

Catalyst	X_{LA} (t = 0)	Selectivities at t = 0								CB (t = 0)	% C
		AD	CO	AA	PA	PD	LA_2	LA_3	LA_4		
HMCM22	100	26.3	13.4	1.5	0	1.8	0	0.7	1.3	45.3	10.8
HZSM5	100	38.0	19.0	0.3	2.5	1.5	1.1	8.2	27.8	98.4	7.9
NaZSM5	100	64.0	32.0	0.5	0	0	0	0.6	0.6	97.7	5.2

All values are in % [583 K, 101.3 kPa total pressure, P_{LA} = 3 kPa, P_{H_2O} = 27 kPa, P_{N_2} = 71.3 kPa, W/F^0_{LA} = 19.3 g h/mol].

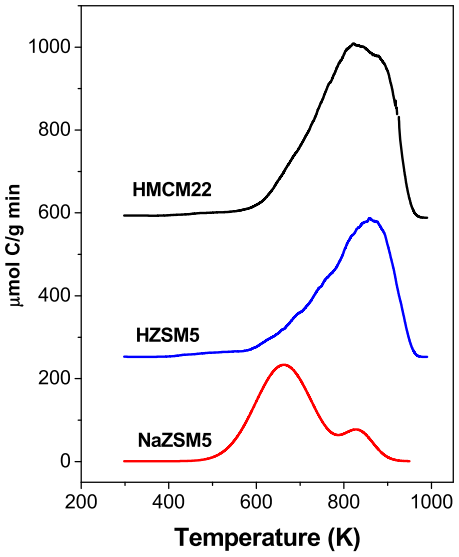

Fig. 6. TPO profiles of samples recovered from the catalytic runs showed in Fig. 5. Heating rate, 10 K/min.

The carbon balance at t = 0 on NaZSM5 was always close to 98%. The initial LA conversion rate on NaZSM5 determined from Fig. 7B was r^0_{LA} = 0.205 mol/g h, comparable to that obtained on HZSM5.

4. Discussion

Among the LA conversion pathways depicted in Fig. 1, the LA decarbonylation to (AD + CO) was preferentially promoted on zeolites HMCM22, HZSM5 and NaZSM5. Nevertheless, the activity/selectivity results showed that they exhibited different catalytic performance for AD synthesis from LA; for example, the maximum (AD + CO) yields ($Y_{(AD+CO)}$) obtained in this work followed the order (Table 2): NaZSM5 (96.0%) > HZSM5 (57.0%) > HMCM22 (39.7%). This $Y_{(AD+CO)}$ trend may be explained by considering the different acidic (acid site nature, density and strength) and physical (pore size) properties of the zeolites.

HMCM22 is a strong acid zeolite that contained the highest acid site density (551 μmol/g) and B/L acid site ratio (4.2), as shown in Table 1. The promotion of the LA decarbonylation to AD pathway on strong protonic sites was observed by Katryniok et al. [6] who reported (AD + CO) yields of up to 83% on silica-supported $H_4SiW_{12}O_{40}$ heteropolyacid catalysts. Xu et al. [35] studied the conversion of methyl lactate on zeolites HY and HZSM5 and reported that the Brønsted acid sites are very efficient at catalyzing methyl lactate decarbonylation to produce acetaldehyde. Similarly, the strong Brønsted acidity may explain here the significant formation of (AD + CO) products obtained on HMCM22 (Table 2). However, strong Brønsted acid sites may also catalyze LA condensation and polymerization reactions, which usually results in a significant coke deposition. In this regard, our results show the LA conversion reaction on HMCM22 forms abundant amounts of coke, and that the carbon balance was very low during the entire catalytic run. Both results are consistent with a rapid LA oligomerization leading to coke formation. It is important noting here that only very small amounts of LA trimers and tetramers were detected among the reaction products on HMCM22, which probably reflects that the narrow 10-member ring sinusoidal channels of HMCM22 (4.0 Å × 5.0 Å) hamper by diffusional constraints the gas-phase diffusion of LA oligomers to the exterior through the zeolite pore system. It seems, therefore, that zeolite HMCM22 is not suitable for selectively producing AD from LA because its strong Brønsted acidity and particular pore architecture promote concomitantly the competitive LA oligomerization pathway.

Zeolite HZSM5 exhibited a high density of surface acid sites (413 μmol/g), preponderantly Brønsted acid sites (B/L ratio = 3.1), and catalyzed at high rate the (AD + CO) formation through LA decarbonylation. At W/F^0_{LA} = 19.3 g h/mol and 583 K, LA was completely converted on HZSM5 yielding at the beginning of the reaction mainly (AD + CO) (57%) and LA oligomers (37.1%) with a good carbon balance (98.4%) (Fig. 5 and Table 2). With the progress of the reaction, the selectivity to (AD + CO) and LA oligomers decreased so that the carbon balance was only 50.3% at the end of the 4-h run. The coke amount formed on HZSM5 was signifi-

Please cite this article in press as: M.E. Sad, et al., Selective synthesis of acetaldehyde from lactic acid on acid zeolites, Catal. Today (2017), http://dx.doi.org/10.1016/j.cattod.2017.03.024

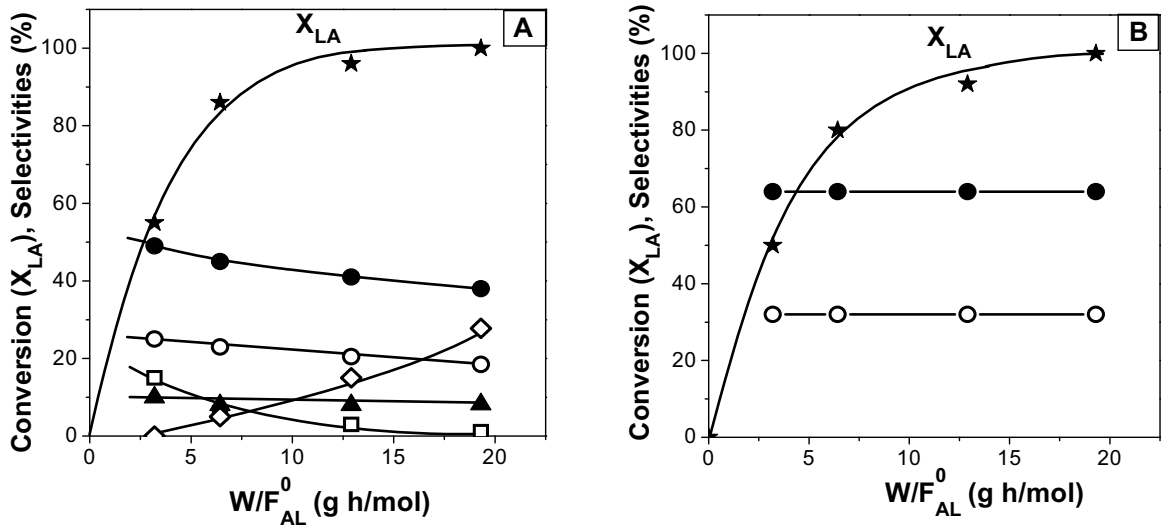

Fig. 7. LA conversion (⋆) and selectivities: AD (●), CO (○), LA_2 (□), LA_3 (▲), LA_4 (◊), as a function of contact time, on HZSM5 (A) and NaZSM5 (B).

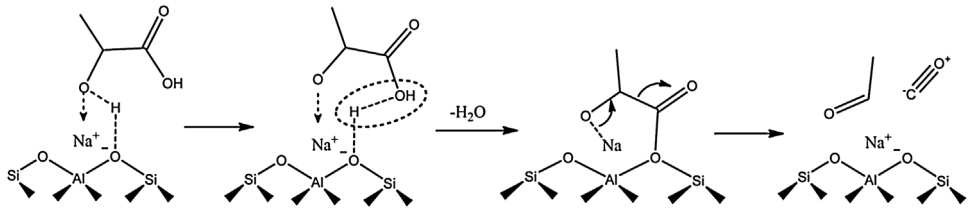

Fig. 8. Probable reaction mechanism for LA decarbonylation to acetaldehyde on NaZSM5.

cant (7.9%). The results in Fig. 7A showed that the formation of LA dimer diminished while that of LA tetramer increased when X_{AL} was increased, thereby reflecting the consecutive formation of heavier oligomers via $LA_2 \rightarrow LA_3 \rightarrow LA_4 \rightarrow LA_n$ where LA_n oligomers ($n > 4$) were not detected in the gas phase and probably remain adsorbed on the surface forming coke precursor species. In summary, all these results obtained on HZSM5 confirm that the strong protonic sites of acid zeolites catalyze preferentially both the LA decarbonylation and LA polymerization reactions.

Zeolite NaZSM5 contained the lowest density of surface acid sites (263 μmol/g), mainly Lewis acid sites (B/L = 0.4) of weak and intermediate strength (Figs. 3 and 4). This zeolite was an excellent catalyst to obtain selectively acetaldehyde by lactic acid decarbonylation. In fact, at W/F^0_{LA} = 19.3 g h/mol and 583 K NaZSM5 converted totally LA, yielded 96% (AD + CO) and formed the lowest amount of coke (5.2%) (Table 2). The selective formation of acetaldehyde on NaZSM5 was observed for the entire contact time range investigated in this work; Fig. 7B shows, in fact, that the (AD + CO) selectivity remained closed to 96% when X_{AL} varied between 50% and 100%. Only very small amounts of LA oligomers were detected during the catalytic runs of Fig. 7B. All these results show that the Lewis Na sites of moderate acid strength present in high concentration on NaZSM5 promote efficiently the LA decarbonylation to AD while suppressing almost completely LA oligomerization. Previous work has reported that bulk alumina may catalyze the decarbonylation of lactates [35]. In order to check if zeolite NaZSM5 contains extra-framework Al species that would promote LA decarbonylation, we characterized this zeolite by NMR technique. The ^{27}Al MAS n.m.r spectrum is presented in the Supporting Information and shows that the Al atoms are in the zeolite structure forming tetrahedral species of $Al(OSi)_4$ configuration; i.e., zeolite NaZSM5 does not contains extra-framework aluminum species. On the other hand, formation of coke was lower on NaZSM5 (%C = 5.2) than on HZM5 (%C = 7.9), probably reflecting that zeolite HZSM5 contains a much higher concentration of stronger Brønsted acid sites than NaZSM5 (Table 1 and Fig. 4).

The reaction mechanism of LA decarbonylation to AD on medium-strength acid sites has been studied on calcium hydroxyapatites [36] and Mg-Al mixed oxides [18]. Based on these studies and the results of the present work, we propose in Fig. 8 a possible reaction mechanism for the synthesis of AD from LA on NaZSM5. Lactic acid would adsorb dissociatively via its hydroxyl group on a Na^+-$O^{\delta-}$ pair of NaZSM5, so that the Na Lewis acid site interacts with the adsorbate forming a C—O—Na bond. The hydroxyl proton is adsorbed on the $O^{\delta-}$ center and reacts with the LA carboxylic group to form after dehydration an ester intermediate that finally decomposes to give AD and CO. It is worth noting that, in contrast with the results obtained here on NaZSM5, other authors have reported that zeolites NaY promote better the lactic acid dehydration to AA than its decarbonylation to AD [35,37]. Our results show that zeolite NaZSM5 formed only very small amounts of AA among the products in our catalytic runs. More studies are needed to achieve a solid mechanistic understanding of lactic acid decarbonylation/dehydration reaction pathways on fully Na exchanged acid zeolites.

5. Conclusions

The selective formation of acetaldehyde from lactic acid on acid zeolites depends on both the zeolite pore structure and the acid site nature and strength. The strong Brønsted acidity of zeolite HMCM22 promotes preferentially the lactic acid decarbonylation to acetaldehyde. Nevertheless, strong Brønsted acid sites and the narrow 10-member ring channels of HMCM22 also favor the rapid formation of significant amounts coke precursors via lactic acid oligomerization. The maximum yield to lactic acid decarbonyla-

Please cite this article in press as: M.E. Sad, et al., Selective synthesis of acetaldehyde from lactic acid on acid zeolites, Catal. Today (2017), http://dx.doi.org/10.1016/j.cattod.2017.03.024

tion products (AD + CO) on HMCM22 at 583 K was therefore only 39.7%. Zeolite HZSM5 converts lactic acid to acetaldehyde at high rates, yielding (AD + CO) products up to 57%, but the strong Brønsted acid sites of this zeolite also promote the competitive lactic acid oligomerization reaction. NaZSM5 contains mainly Lewis acid sites of weak and intermediate strength that promote efficiently the formation of acetaldehyde while suppressing almost completely lactic acid oligomerization. Zeolite NaZSM5 is therefore an excellent catalyst to selectively obtain acetaldehyde through lactic acid decarbonylation, yielding (AD + CO) products up to 96% with an AD/CO carbon ratio of two.

Acknowledgements

We thank the Universidad Nacional del Litoral (UNL), the Agencia Nacional de Promoción Científica y Tecnológica (ANPCyT) and CONICET, Argentina, for the financial support of this work.

Appendix A. Supplementary data

Supplementary data associated with this article can be found, in the online version, at http://dx.doi.org/10.1016/j.cattod.2017.03.024.

References

[1] J.E. Bailey, M. Bohnet, J. Brinker, Ullman's Encyclopedia of Industrial Chemistry, 6th ed., Willey-VCH, Weinheim, 2005.
[2] K. Weissermel, H.J. Arpe, Industrial Organic Chemistry, 3rd ed., Wiley-VCH, Weinheim, 1997.
[3] R. Jira, Angew. Chem. Int. Ed. 48 (2009) 9034–9037.
[4] P. Liu, E.J.M. Hensen, J. Am. Chem. Soc. 135 (2013) 14032–14035.
[5] Y. Guan, E.J.M. Hensen, J. Catal. 305 (2013) 135–145.
[6] B. Katryniok, S. Paul, F. Dumeignil, Green Chem. 12 (2010) 1910–1913.
[7] C.M. Tang, J.S. Peng, X.L. Li, Z.J. Zhai, W. Bai, N. Jiang, H. Gao, Y. Liao, Green Chem. 17 (2015) 1159–1166.
[8] R. Datta, M. Henry, J. Chem. Technol. Biotechnol. 81 (2006) 1119–1129.
[9] F.A. Castillo Martinez, E.M. Balciunas, J.M. Salgado, J.M. Dominguez Gonzalez, A. Converti, R. Pinheiro de Souza Oliveira, Trends Food Sci. Technol. 30 (2013) 70–83.
[10] T.L. Turner, G.C. Zhang, S.R. Kim, V. Subramaniam, D. Steffen, Ch.D. Skory, J.Y. Jang, B.J. Yu, Y.S. Jin, Appl. Microbiol. Biotechnol. 99 (2015) 8023–8033.
[11] J.C. Serrano-Ruiz, J.A. Dumesic, ChemSusChem 2 (2009) 581–586.
[12] J.J. Bozell, G.R. Petersen, Green Chem. 12 (2010) 539–554.
[13] D. Garlotta, J. Polym. Environ. 9 (2002) 63–84.
[14] Y. Fan, C. Zhou, X. Zhu, Catal. Rev. 51 (2009) 293–324.
[15] P. Sun, D. Yu, K. Fu, M. Gu, Y. Wang, H. Huang, H. Ying, Catal. Commun. 10 (2009) 1345–1349.
[16] B. Yan, L.Z. Tao, Y. Liang, B.Q. Xu, ChemSusChem 7 (2014) 1568–1578.
[17] Z. Zhai, X. Li, C. Tang, J. Peng, N. Jiang, W. Bai, H. Gao, Y. Liao, Ind. Eng. Chem. Res. 53 (2014) 10318–10327.
[18] C. Tang, Z. Zhai, X. Li, L. Sun, W. Bai, J. Catal. 329 (2015) 206–217.
[19] M.K. Rubin, P. Chu, US Patent 4,954,325, 1990.
[20] B.C. Lippens, B.G. Linsen, J.H. De Boer, J. Catal. 3 (1964) 32–37.
[21] W.D. Harkins, G. Jura, J. Chem. Phys. 11 (1943) 431–432.
[22] M.E. Sad, C.L. Padró, C.R. Apesteguía, J. Mol. Catal. A: Chem. 327 (2010) 63–72.
[23] P.A. Jacobs, R. von Ballmoos, J. Phys. Chem. 86 (1982) 3050–3053.
[24] M.T. Aronson, R.J. Gorte, W.E. Farneth, J. Catal. 105 (1987) 455–468.
[25] C.L. Padró, C.R. Apesteguía, J. Catal. 226 (2004) 308–320.
[26] E.P. Parry, J. Catal. 2 (1963) 371–379.
[27] J.W. Ward, J. Catal. 10 (1968) 34–46.
[28] H. Knözinger, Adv. Catal. 25 (1976) 184–271.
[29] G. Busca, Catal. Today 41 (1998) 191–200.
[30] S. Khabtou, T. Chevreau, J.C. Lavalley, Microporous Mater. 3 (1994) 133–148.
[31] C.A. Emeis, J. Catal. 141 (1993) 347–354.
[32] D. Meloni, S. Laforge, D. Martin, M. Guisnet, E. Rombi, V. Solinas, Appl. Catal. A 215 (2001) 55–66.
[33] A. Corma, C. Corell, V. Fornés, W. Kolodziejski, J. Pérez-Pariente, Zeolites 15 (1995) 576–582.
[34] M.E. Sad, C.L. Padró, C.R. Apesteguía, Appl. Catal. A: Gen. 342 (2008) 40–48.
[35] B.M. Murphy, M.P. Letterio, B. Xu, J. Catal. 339 (2016) 21–30.
[36] V.C. Ghantani, S.T. Lomate, M.K. Dongare, S.B. Umbarkar, Green Chem. 15 (2013) 1211–1217.
[37] J. Zhang, Y. Zhao, M. Pan, X. Feng, W. Ji, C.T. Au, ACS Catal. 1 (2011) 32–41.